Cell Reports

Report

Defined MicroRNAs Induce Aspects of Maturation in Mouse and Human Embryonic-Stem-Cell-Derived Cardiomyocytes

Graphical Abstract

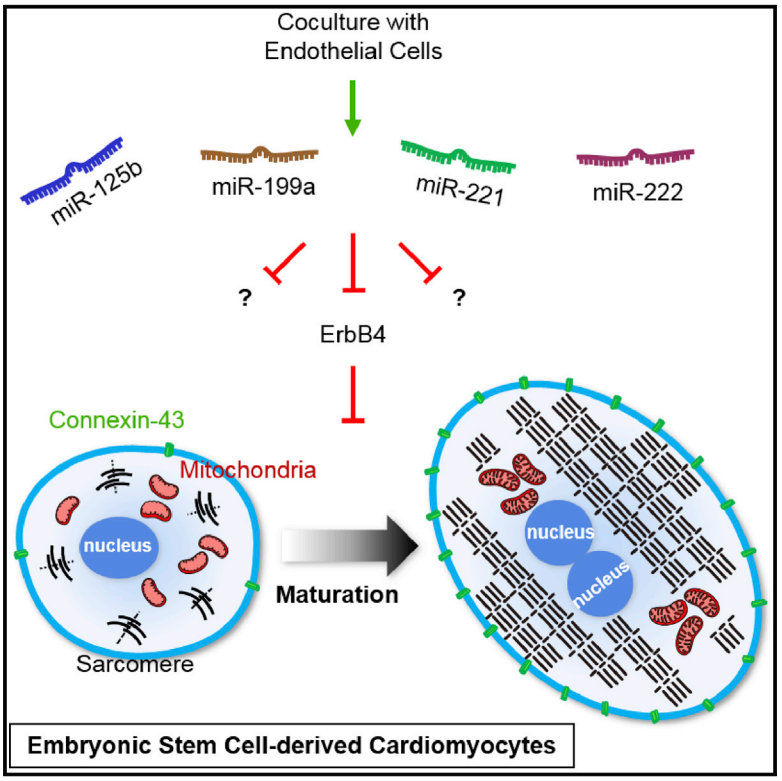

Authors

Desy S. Lee, Jyh-Hong Chen, David J. Lundy, ..., Shu Chien, Charles E. Murry, Patrick C.H. Hsieh

Correspondence

phsieh@ibms.sinica.edu.tw (P.C.H.H.), jyhhong@mail.ncku.edu.tw (J.-H.C.)

In Brief

Lee et al. report that coculture of embryonic stem cell (ESC)-derived cardiomyocytes with endothelial cells enhances ESC-CM maturity and upregulates several microRNAs. Delivery of selected microRNAs phenocopies this effect, allowing for improved in vitro maturation of ESC-derived cardiomyocytes.

Highlights

- Coculture of ESC-CMs with endothelial cells improves features of ESC-CM maturation
- Transfection of four miRNAs phenocopies this effect in mouse and human ESC-CMs
- This miRNA combination targets ErbB4

Accession Numbers

GSE69927
GSE69897

Lee et al., 2015, Cell Reports *12*, 1960–1967
September 29, 2015 ©2015 The Authors
http://dx.doi.org/10.1016/j.celrep.2015.08.042

CellPress

OPEN ACCESS
CellPress

Cell Reports
Report

Defined MicroRNAs Induce Aspects of Maturation in Mouse and Human Embryonic-Stem-Cell-Derived Cardiomyocytes

Desy S. Lee,[1,2] Jyh-Hong Chen,[3,*] David J. Lundy,[2] Chung-Hung Liu,[2] Shiaw-Min Hwang,[4] Lil Pabon,[5] Ru-Chi Shieh,[2] Chien-Chang Chen,[2] Sheng-Nan Wu,[6] Yu-Ting Yan,[2] Sho-Tone Lee,[2] Po-Min Chiang,[1] Shu Chien,[7] Charles E. Murry,[5,8,9] and Patrick C.H. Hsieh[1,2,8,10,*]

[1]Institute of Clinical Medicine, National Cheng Kung University, Tainan 704, Taiwan
[2]Institute of Biomedical Sciences, Academia Sinica, Taipei 115, Taiwan
[3]Department of Medicine, National Cheng Kung University, Tainan 704, Taiwan
[4]Bioresource Collection and Research Center, Food Industry Research and Development Institute, Hsinchu 300, Taiwan
[5]Department of Pathology, Center for Cardiovascular Biology, Institute for Stem Cell and Regenerative Medicine, University of Washington, Seattle, WA 98109, USA
[6]Department of Physiology, National Cheng Kung University, Tainan 704, Taiwan
[7]Department of Bioengineering, University of California at San Diego, San Diego, CA 92093, USA
[8]Department of Bioengineering, University of Washington, Seattle, WA 98109, USA
[9]Department of Medicine/Cardiology, University of Washington, Seattle, WA 98109, USA
[10]Division of Cardiovascular Surgery, National Taiwan University Hospital, Taipei 100, Taiwan
*Correspondence: phsieh@ibms.sinica.edu.tw (P.C.H.H.), jyhhong@mail.ncku.edu.tw (J.-H.C.)
http://dx.doi.org/10.1016/j.celrep.2015.08.042

SUMMARY

Pluripotent-cell-derived cardiomyocytes have great potential for use in research and medicine, but limitations in their maturity currently constrain their usefulness. Here, we report a method for improving features of maturation in murine and human embryonic-stem-cell-derived cardiomyocytes (m/hESC-CMs). We found that coculturing m/hESC-CMs with endothelial cells improves their maturity and upregulates several microRNAs. Delivering four of these microRNAs, miR-125b-5p, miR-199a-5p, miR-221, and miR-222 (miR-combo), to m/hESC-CMs resulted in improved sarcomere alignment and calcium handling, a more negative resting membrane potential, and increased expression of cardiomyocyte maturation markers. Although this could not fully phenocopy all adult cardiomyocyte characteristics, these effects persisted for two months following delivery of miR-combo. A luciferase assay demonstrated that all four miRNAs target ErbB4, and siRNA knockdown of ErbB4 partially recapitulated the effects of miR-combo. In summary, a combination of miRNAs induced via endothelial coculture improved ESC-CM maturity, in part through suppression of ErbB4 signaling.

INTRODUCTION

Cells differentiated from embryonic stem cells (ESCs) and induced pluripotent stem cells (iPSCs) could form ideal platforms for in vitro disease modeling and the development and testing of new therapeutics. These tools are of importance in fields in which primary human cells and tissues are not readily available, such as in cardiac or neurological research. However, one major obstacle is that cells derived from ESCs/iPSCs are generally immature and tend to display the structural and functional attributes of fetal cells, rather than the adult phenotype (Blum et al., 2012; Maroof et al., 2013; Yang et al., 2014a).

Cardiac disease is one of the severe causes of morbidity and mortality in the world (Lloyd-Jones et al., 2010). To this end, several groups have developed protocols for differentiating pluripotent stem cells into cardiomyocytes (CMs). However, these differentiated cells remain immature in both morphology and performance. This is not surprising, given that neonatal human cardiomyocytes require many years of maturation in vivo before fully adopting the adult phenotype, whereas ESC/iPSC-CM are differentiated for only a matter of weeks (Peters et al., 1994). An immature pluripotent-cell-derived cardiomyocyte exhibits a round cell shape, a disorganized contractile apparatus, a single nucleus, limited calcium-handling ability, and a resting membrane potential of around –60 mV. In contrast, a mature adult cardiomyocyte is significantly larger, is rod-shaped, has highly organized sarcomeres, has polarized connexin-43 (Cx-43), and has a more negative resting potential of around –90 mV. A larger proportion of cells are also multinucleated (Yang et al., 2014a). A fully mature cardiomyocyte also shows regularly spaced transverse tubules (T tubules), which are essential for proper excitation-contraction coupling with even distribution of action potentials (Ziman et al., 2010).

Due to these structural and functional differences, cardiomyocytes that have been differentiated from pluripotent stem cells in vitro may be unreliable when used for disease modeling, drug screening, or cell-based therapies (Kim et al., 2013; Laflamme

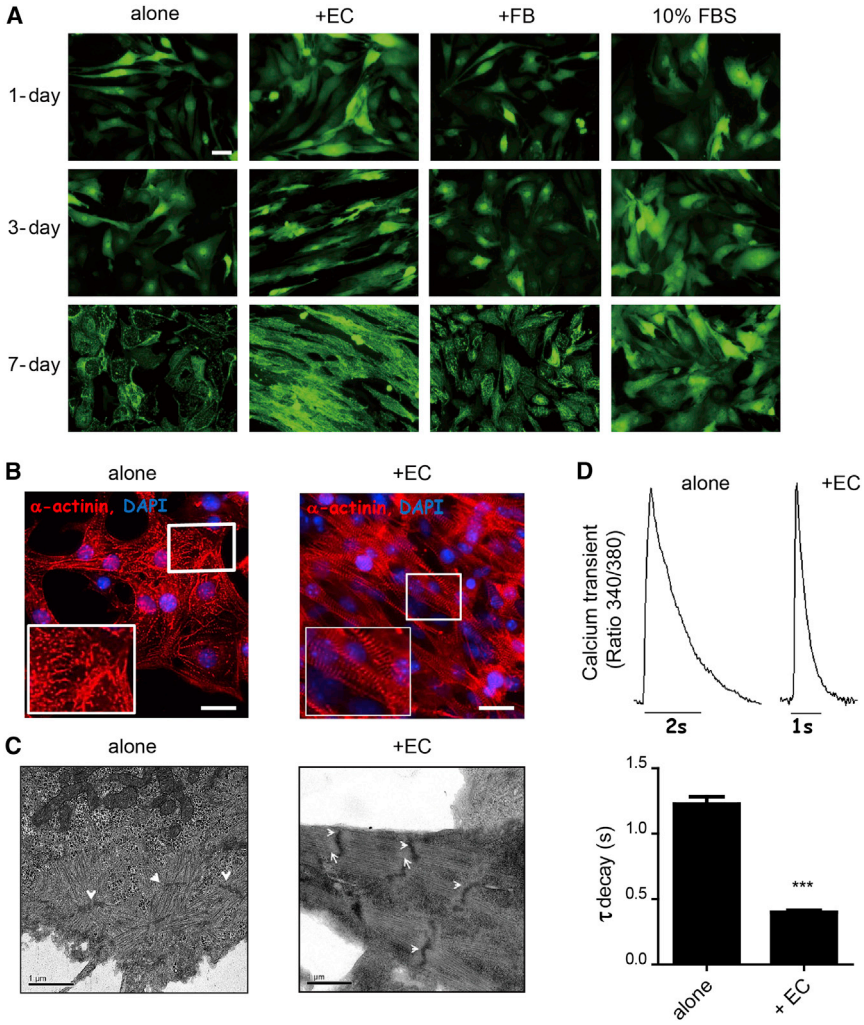

Figure 1. Coculture with Endothelial Cells Enhances Aspects of ESC-Derived Cardiomyocyte Maturation and Upregulates Four MicroRNAs

(A) Mouse embryonic-stem-cell-derived cardiomyocytes (mESC-CMs) were cultured alone in 2% (left), 10% (right) FBS, or with endothelial cells (+EC) or fibroblasts (+FB) for 1, 3, or 7 days. Scale bar, 50 μm; green, α-MHC (EGFP).

(B) Immunofluorescence staining of mESC-CMs cultured alone or with ECs at day 3. Red, α-sarcomeric actinin (α-actinin); blue, DAPI. Scale bar, 25 μm.

(C) Ultrastructural images showing sarcomere structure of mESC-CMs after 3 days of coculture with ECs (arrowhead, Z disk; arrow, I band). Scale bar, 1 μm.

(D) Representative tracing of spontaneous Ca^{2+} transients of mESC-CMs cultured alone or with ECs at day 3. The time constant of Ca^{2+} transient decay, characterizing the speed of recovery, was quantified in each group.

Means ± SEM are shown. For statistical data, at least $n \geq 3$; ***$p < 0.001$.

See also Figure S1.

RESULTS

Coculture with Endothelial Cells Induces Aspects of Maturation in Mouse Embryonic-Stem-Cell-Derived Cardiomyocytes

Mouse embryonic stem cells (mESCs) stably transfected with a cardiac-specific alpha-MHC-driven EGFP reporter (Takahashi et al., 2003) were differentiated into cardiomyocytes (CMs) using the hanging drop method; this yielded ~15% mESC-CMs (Figures S1A and S1B). These mESC-CMs were purified by fluorescence-activated cell sorting (FACS) and cocultured with rat endothelial cells (ECs) (Figure S1C) or mouse cardiac fibroblasts, which had been previously seeded on the plate. We observed that mESC-CMs cocultured with ECs took on an elongated cell shape and improved their alignment, compared to when they were cultured alone or with fibroblasts (Figure 1A).

During development, rodent heart maturation is characterized by a switch of fetal-specific myosin heavy-chain β-isoform (β-MHC) to the α-isoform (α-MHC) that is predominantly expressed in adult rodent hearts (Lompré et al., 1984). ESC-CMs were sorted from coculture by FACS, based on an $EGFP^+$ signal, and the *α-/β-MHC* ratio was assessed by quantitative real-time PCR. We found a higher α-/β-MHC ratio in ESC-CMs that had been cocultured with ECs, compared to ESC-CMs cultured alone (Figure S1E), reflecting a change of ESC-CM maturity following coculture.

Both immunofluorescence and ultrastructural analyses of cocultured mESC-CMs revealed myofibrils with properly aligned Z bands, whereas ESC-CMs cultured alone contained only nascent myofibrils and poorly aligned, immature Z-bodies

and Murry, 2005; Navarrete et al., 2013; Yang et al., 2014a). Given that previously undetected cardiac toxicity is one of the leading causes of drug development failure, the problem appears to be significant (Navarrete et al., 2013). Thus, the need for mature ESC/iPSC-CMs is clearly recognized, and many groups have attempted to improve ESC/iPSC-CM maturation by a variety of methods (Kim et al., 2010; Kuppusamy et al., 2015; Nunes et al., 2013; Yang et al., 2014b).

It is known that the function of cardiomyocytes is considerably dependent on endothelial cells (Brutsaert, 2003; Hsieh et al., 2006a) and that endothelial cells play a role in promoting cardiomyocyte survival and organization (Hsieh et al., 2006b). In our study, we found an increase of a group microRNAs (miRNAs) when ESC-CMs were cocultured with endothelial cells. miRNAs, a group of small noncoding RNAs that post-transcriptionally repress the expression of their target genes in a sequence-specific manner, have profound effects in orchestrating cardiac development, function, and pathological responses to injury (Cordes and Srivastava, 2009; Small et al., 2010). In this report, we sought to determine whether miRNAs play a role in ESC-CM maturation during coculture with endothelial cells.

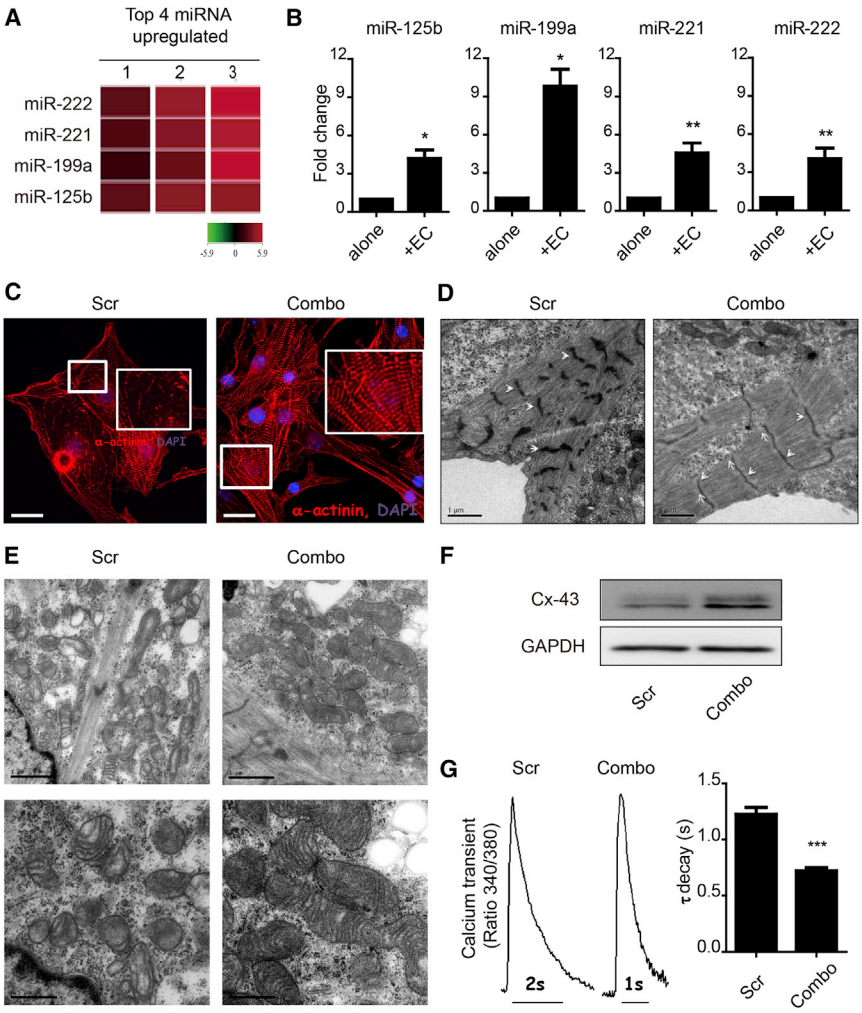

Figure 2. Defined MicroRNAs Promote Several Maturation-Associated Changes in mESC-CMs

(A) Heatmap showing the four most significantly upregulated miRNAs upon coculture from three independent experiments.

(B) Confirmation of upregulated miRNAs in mESC-CMs using quantitative real-time PCR. EGFP$^+$ cells were sorted from the coculture system before analysis.

(C) Immunofluorescence staining showing α-sarcomeric actinin (α-actinin; red) and DAPI (blue) in mouse ESC-CMs transfected with pre-Scr or miR-combo after 3 days. Scale bar, 25 μm.

(D) Representative ultrastructural images of mESC-CMs transfected with pre-Scr or miR-combo after 3 days showing sarcomere organization (arrowhead, Z disk; arrow, I band). Scale bar, 1 μm.

(E) Representative ultrastructural images of mitochondria in mESC-CMs 3 days following transfection with pre-Scr or miR-combo. Scale bar, 1 μm (top), 0.5 μm (bottom).

(F) A western blot shows Cx-43 in mESC-CMs transfected with pre-Scr or miR-combo after 3 days. GAPDH was used as loading control.

(G) Representative tracing of spontaneous Ca^{2+} transients of mESC-CMs transfected with pre-Scr or miR-combo after 3 days. The time constant of Ca^{2+} transient decay, characterizing the speed of recovery, was quantified in each group.

Means ± SEM are shown. For statistical data, at least $n \geq 3$; *$p < 0.05$, **$p < 0.01$, ***$p < 0.001$. See also Figures S2 and S3.

(Figures 1B and 1C). I bands, a marker of the mature phenotype, could only be visualized in the EC coculture group (Figure 1C). Calcium oscillations may also be used to characterize the maturity of pluripotent-cell-derived cardiomyocytes. Therefore, we measured calcium oscillations of cocultured ESC-CMs using Fura-2, a Ca^{2+}-sensitive dye. The rising slope and time to peak were not significantly different between the two groups; however, a faster τ decay indicates improved kinetics of Ca^{2+} clearance from the cytosol of ESC-CMs cultured with ECs (Figure 1D). These data were supported by the elevation of the sarcoplasmic reticulum Ca^{2+} ATPase, *Serca2a* in cocultured ESC-CMs (Figure S1F).

Delivery of Four MicroRNAs Induces Several Maturation-Associated Changes in Mouse ESC-CMs

In order to compare miRNA expression profiles between ECs cocultured ESC-CMs and those cultured alone, we used FACS to isolate ESC-CMs from coculture before extracting RNA and performing an miRNA microarray (Figure S2A). We chose candidates that were most differentially upregulated in EC-cocultured ESC-CMs in three independent experiments: these were *miR-125b-5p*, *miR-199a-5p*, *miR-221*, and *miR-222* (Figure 2A). The expression levels of these miRNAs were then confirmed using quantitative real-time PCR (Figures 2B and S2B). Interestingly, these miRNAs also showed elevation during the embryonic stage of murine heart development (Figure S2C). All of these miRNAs have been previously linked to cardiovascular disease in different roles (Cardinali et al., 2009; Ge et al., 2011; Small et al., 2010; van Rooij et al., 2006; Wong et al., 2012).

Next, we tested each of these miRNAs in gain-of-function assays using synthetic miRNA precursors (Figure S3A), using the switch from β-MHC to α-MHC as a marker of maturation. Transfecting individual miRNAs had no significant effect on the *α-/β-MHC* ratio (Figure S3B). However, since it has been reported that the combined overexpression of miRNAs is necessary to exert their particular function (Hu et al., 2011; Miyoshi et al., 2011), we reasoned that the addition of these four miRNAs together (miR-combo) may be necessary to exert their effects. As suspected, a significant enhancement of the *α-/β-MHC* ratio was seen in ESC-CMs transfected with miR-combo (Figure S3B), reflecting a more mature phenotype. On the basis of these findings, we used these four miRNAs in combination for further experiments.

Next, we wanted to examine whether transfection with miR-combo could replicate the changes in mESC-CM morphology

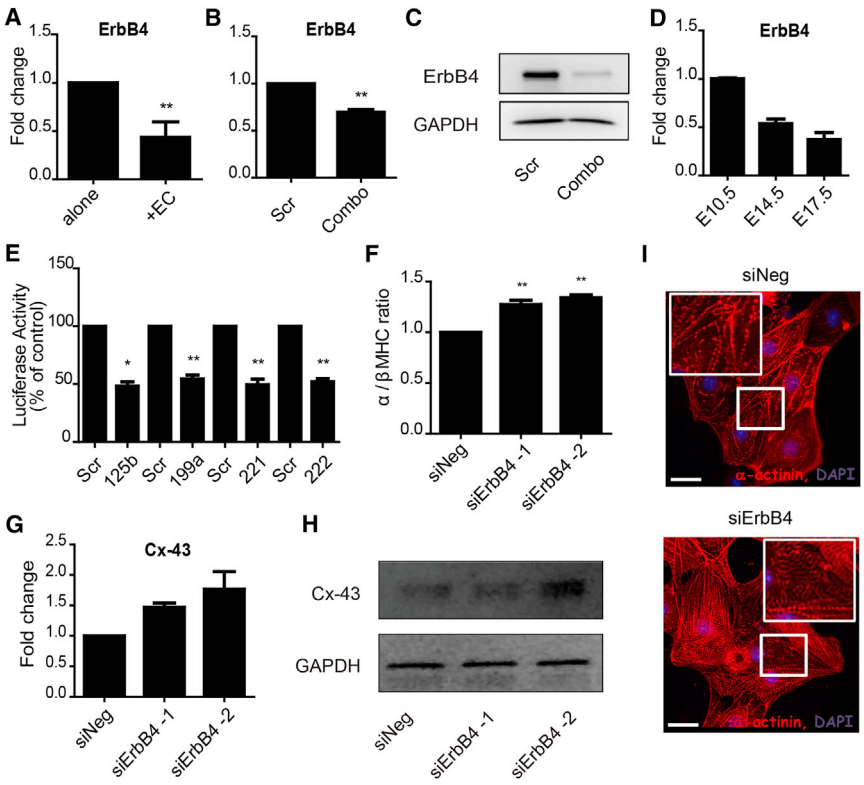

Figure 3. ErbB4 as a Common Target of miR-Combo

(A) The expression of *ErbB4* was characterized in mESC-CMs using quantitative real-time PCR. EGFP^{+} mESC-CMs were sorted from cocultures before analysis.

(B) The expression of *ErbB4* was examined in mESC-CMs 48 hr following miR combo transfection.

(C) A western blot shows the protein level of ERBB4 in hESC-CMs after miR combo delivery. GAPDH is shown as a loading control.

(D) The expression pattern of *ErbB4* was determined in mouse heart at E10.5, E14.5, and E17.5 using quantitative real-time PCR.

(E) A luciferase reporter assay 48 hr post-transfection shows that each miRNA targets the *ErbB4* 3′ UTR.

(F) The α-*to*-β*MHC* ratio was examined in mESC-CMs transfected with *ErbB4* siRNA, relative to siNeg (negative control) after 3 days. Data were normalized to *GAPDH*.

(G) The *Cx-43* gene level was determined in mESCMs transfected with *ErbB4* siRNA, shown relative to siNeg after 3 days. Data were normalized to *GAPDH*.

(H) A western blot shows the protein level of Cx-43 in mESC-CMs transfected with siNeg, siErbB4-1, or siErbB4-2 after 3 days.

(I) Immunofluorescence staining for α-sarcomeric actinin (α-actinin; red) and DAPI (blue) in mESC-CMs transfected with siNeg and siErbB4. Scale bar, 25 μm.

Means ± SEM are shown. For statistical data, at least $n \geq 3$; $^{*}p < 0.05$, $^{**}p < 0.01$. See also Figure S4.

and calcium handling that we observed during coculture with endothelial cells. Indeed, miR-combo-transfected mESC-CMs showed a more elongated structure than scramble-transfected controls (Figure S3C) and contained more aligned, mature myofibrils in the cytoplasm (Figures 2C and S3D), similar to those observed during EC coculture. miR-combo-transfected mESC-CMs also showed more organized sarcomeric structures with the presence of I bands (Figures 2D and S3E) and mitochondrial inner membranes with more well-formed cristae (Figures 2E and S3F). In addition, an increased protein level of the cardiomyocyte gap junction component Cx-43 was also measured (Figure 2F). An examination of calcium transients revealed a significant increase in the decay rate of Ca^{2+} clearance, as evidenced by a decrease in τ decay time (Figure 2G). All of these findings point to an improvement in the maturity status of mESC-CM following miR-combo delivery.

ErbB4 is Downregulated following EC Coculture and miR-Combo Delivery

miRNAs are known to post-transcriptionally repress the expression of target genes. Therefore, we carried out target prediction analysis of *miR-125b-5p*, *miR-199a-5p*, *miR-221*, and *miR-222* using TargetScan. TargetScan revealed that the 3′ UTR of *ErbB4* is a common target of these four miRNAs (Figure S4A). Indeed, we confirmed that there is a significant reduction in the expression of *ErbB4* in ESC-CMs following EC coculture and following miR-combo delivery (Figures 3A–3C). *ErbB4* expression was also found to decline during the prenatal stage of cardiac development, inversely correlated with the expression of these four miRNAs (Figure 3D). In order to verify that these miRNAs can indeed target *ErbB4*, we cloned the *ErbB4* 3′ UTR sequence and ligated it behind the luciferase gene. We found that each individual miRNA can significantly reduce luciferase activity, suggesting that each miRNA in the miR-combo can target *ErbB4* (Figure 3E).

Since miR-combo treatment appears to target *ErbB4* expression, we sought to examine whether the same maturation-associated changes could be observed following knockdown of *ErbB4*. Therefore, ESC-CMs were transfected with two different *ErbB4* small interfering RNA (siRNAs) (Figure S4B), and we used the same assays to assess the maturity indices of each group. We found a higher α-/β-*MHC* ratio (Figure 3F), increased gene and protein expression of Cx-43 (Figures 3G and 3H), and more aligned sarcomeres following *ErbB4* knockdown (siErbB4; Figure 3I). Notably, the degree of ESC-CM maturity correlated with the knockdown efficiency of *ErbB4* by the two different siRNAs, with the more efficient siRNA achieving the more mature characteristics. Overall, these data indicate that knockdown of *ErbB4*, as a target of miR-combo, alters many aspects of ESC-CM morphology, gene expression, and protein expression, in accordance with a more mature phenotype.

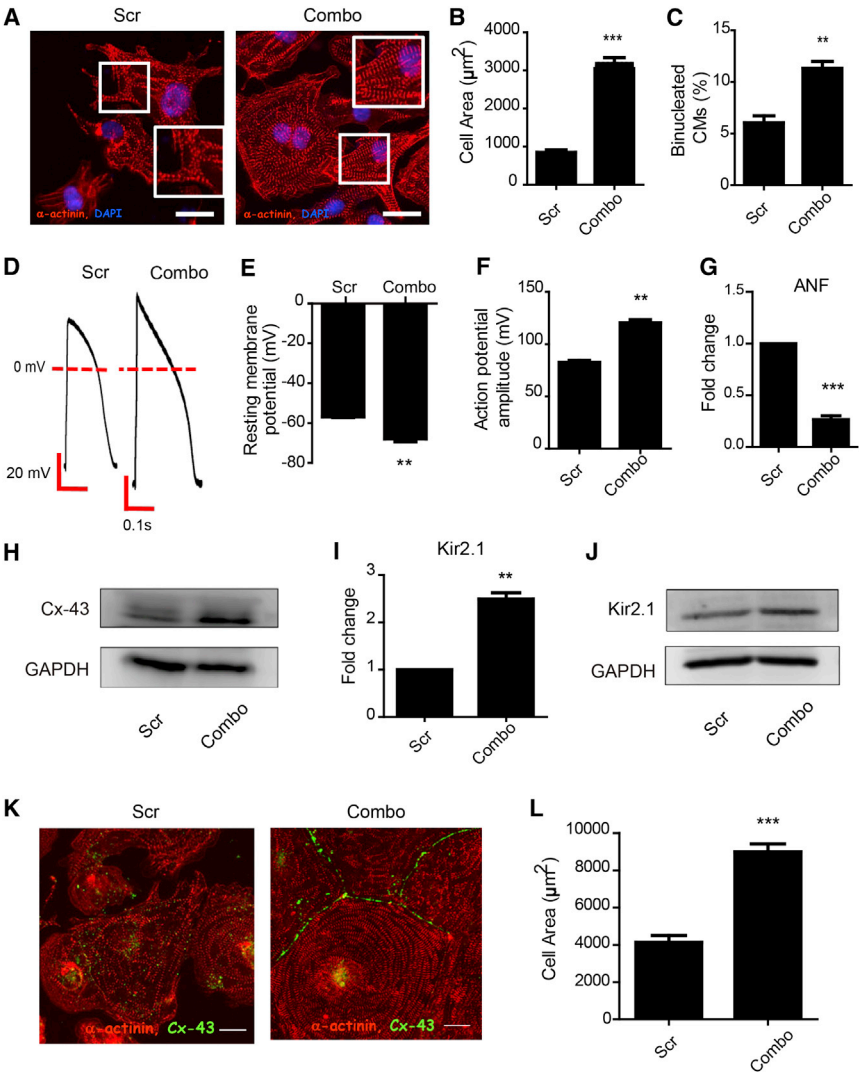

Figure 4. Defined MicroRNAs Change hESC-CM Characteristics in Accordance with Enhanced Maturation

(A) Immunofluorescence staining for α-sarcomeric actinin (α-actinin; red) and DAPI (blue) in human ESC-CMs transfected with pre-Scr or miR-combo. Scale bar, 25 μm.

(B) Quantification of average hESC-CM cell area 3 weeks post transfection with pre-Scr or miR-combo.

(C) Quantification of binucleated hESC-CMs after transfection with pre-Scr or miR-combo after 3 weeks.

(D) Representative recording of action potentials in hESC-CMs 3 weeks post-transfection with pre-Scr or miR-combo.

(E) Quantification of recorded resting membrane potentials (MDPs).

(F) Quantification of recorded action potential amplitude (APA).

(G) The expression of *ANF* was examined in hESC-CMs overexpressed with pre-Scr or miR-combo.

(H) The protein level of Cx-43 was determined by western blot in hESC-CMs. GAPDH was used as a loading control.

(I) The expression of *KIR2.1* was examined in hESC-CMs 1 month post-transfection with pre-Scr or miR-combo.

(J) The protein level of KIR2.1 was determined by western blot in hESC-CMs. GAPDH was used as a loading control.

(K) Representative immunofluorescence staining for α-sarcomeric actinin (α-actinin; red) and Cx-43 (green) in hESC-CMs transfected with pre-Scr or miR-combo. Scale bar, 20 μm.

(L) Quantification of cell area of hESC-CMs after transfection with pre-Scr or miR-combo after 2 months.

Means ± SEM are shown. For statistical data, at least $n \geq 3$; $^{**}p < 0.01$, $^{***}p < 0.001$.

miR-Combo Promotes Several Maturation-Associated Changes in Human ESC-CMs

Human adult cardiomyocytes are an essential tool for scientific research, disease modeling, and drug discovery, yet obtaining primary cells for research is exceedingly difficult. Since *miR-125b-5p*, *miR-199a-5p*, *miR-221*, and *miR-222* are all evolutionarily conserved between mice and humans, we aimed to examine whether our findings from murine ESCs could also apply to the human system. Therefore, we induced cardiac differentiation of H9 ESCs (Yang et al., 2014b) and carried out an extensive characterization of hESC-CM maturity following miR-combo delivery. In a similar manner to mESC-CMs, hESC-CMs showed several morphological changes associated with increased maturation. hESC-CMs transfected with miR-combo showed more organized sarcomeres, a larger cell area, and a higher binucleation ratio compared to scramble miRNA-transfected controls, although they still retained a round cell shape (Figures 4A–4C). These changes were also accompanied by a more negative resting membrane potential and a larger amplitude of action potential, as measured by whole-cell patch clamp (Figures 4D–4F), although still falling short of the electrophysiological performance expected from adult human cardiomyocytes. In addition, we examined the expression level of several genes and proteins that are known to be differently expressed in fetal and adult CMs. Our data show lower expression of *ANF* and higher expression of Cx-43 and KIR2.1 following miR-combo delivery (Figures 4G–4J). All of these factors indicate that hESC-CM take on a more mature phenotype following miR-combo delivery.

In order to form a useful platform for future research, ESC-CMs would ideally show a long-term improvement in maturation, rather than a transient effect. Therefore, we sought to investigate the effects of miR-combo delivery after a longer culture period. We followed hESC-CMs for 2 months after one single transfection with miR-combo and found that, after 2 months, a more organized distribution of Cx-43 and enlarged cell size were still clearly visible in miR-combo-treated hESC-CMs, compared to controls that were cultured for the same period of time (Figures 4K and 4L).

DISCUSSION

Our findings provide a simple and rapid method for enhancing the maturity of murine and human pluripotent-cell-derived CMs in vitro. Although we could not fully recapitulate the adult phenotype (i.e., rod-shaped cells with a resting potential –90 mV, peak action potential of 300 mV, and T tubules), delivery of miR-combo yields a population of cells that display many more aspects of maturation than cells cultured under standard conditions. This method has a number of advantages. First, it is based on real physiological mechanisms, with clues taken from the interactions occurring between cardiac endothelial cells and cardiomyocytes. Second, miRNAs have the potential to regulate many targets and complex pathways to derive their effects, yet they are still more selective than small molecules. Third, miRNAs are easily manipulated ex vivo and so are ideal for increasing in vitro maturation of ESC-CMs. Finally, these effects were demonstrated to persist for at least 2 months after a single miR-combo delivery.

Given the heterogeneity of ECs, we sought to determine whether different ESC-CM maturation effects could be triggered by different sources of ECs upon coculture. Surprisingly, we found that, regardless of origin (heart, fat, or aorta) or even species (mouse, rat, pig, or human), ECs could enhance the maturity of ESC-CMs using the coculture system. In addition, this effect could not be replicated by coculture with fibroblasts (Figures S1D and S1E). Therefore, we postulate that it is a common property of the various ECs that contributes to the maturation effect of ESC-CMs.

We sought to shed light on how coculture with ECs increases the level of miRNAs in ESC-CMs under a variety of conditions. ESC-CMs were cultured in EC-conditioned medium, with a lysate of freeze-thawed ECs, or on an extracellular matrix that had been laid down by ECs. Interestingly, we found that only the lysate of endothelial cells was able to significantly enhance expression of these four miRNAs (Figure S2D). ESC-CMs cultured with EC-conditioned medium or on matrix alone showed only an immature phenotype, whereas ESC-CMs cultured with EC lysate showed much more organized sarcomeric structures (Figure S2E). This would indicate that the main maturation-enhancing effect is not derived through a secreted factor or via any matrix-driven effect. It is known that miRNAs can be transferred directly between cells through gap junctions (Katakowski et al., 2010), and we speculate that this may be the mechanism by which EC coculture affects ESC-CM miRNA concentrations. The precise nature of this interplay requires further investigation, which we aim to carry out in the future.

In terms of the mechanism underlying miR-combo-driven maturation, we found that all four of these miRNAs can independently repress *ErbB4* and that expression of these four miRNAs increases during cardiac development (Figures S2C and S3D). This correlates with a previous report showing that *ErbB4* expression is downregulated during heart development (Zhao et al., 1999). In order to provide insight into the impact of *ErbB4* knockdown, we carried out microarray analysis following siErbB4-2 delivery to ESC-CMs. Gene ontology analysis revealed that genes related to the regulation of transcription, cell differentiation, organelle organization, and ion binding were upregulated. We then chose several potentially relevant genes (*Tuba3a*, *Nefl*, *S100 g*, and *Cyp26a1*) and confirmed their upregulation by quantitative real-time PCR (Figures S4C and S4D). We believe that further analysis of these targets, and others determined during microarray analysis, should be investigated for future studies into the mechanisms underlying ESC-CM maturation.

Previous studies have shown that ErbB4 overexpression can induce postnatal cardiomyocytes to proliferate and re-enter the cell cycle, whereas ErbB4 inactivation suppresses it (Bersell et al., 2009). In addition, an inverse relationship between cardiomyocyte proliferation and maturation has been shown previously (Yang et al., 2014b; Zhang et al., 2010). To this end, we believe that further study using pharmacological inhibition of ErbB4, or indeed inhibition of cell proliferation, and examining the effect on cardiomyocyte maturation would be of interest for future investigation. However, since it is known that miRNAs govern many functional pathways by targeting multiple genes, we do not rule out the possibility that these miRNAs might affect targets other than ErbB4 in mediating the maturation of ESC-CMs.

In summary, we believe that our study has generated a valuable way to enhance the maturation of ESC-CMs in vitro. Although no existing technique, including ours, is able to fully imitate the adult cardiomyocyte phenotype, we hope that this technique can improve the usefulness of pluripotent-stem-cell-derived cardiomyocytes in a variety of applications and that a similar approach will prove useful in other ESC/iPSC-derived cells.

EXPERIMENTAL PROCEDURES

Routine Culture and Cardiac Differentiation of Mouse ESCs

A cardiac-specific α-MHC-driven EGFP reporter was stably transfected in mESCs using a retroviral vector (Takahashi et al., 2003). Cardiac differentiation was induced using the hanging drop technique with ascorbic acid (Sigma, 100 μmol/l). On days 7–10, EGFP-positive ESC-CMs were isolated and sorted by FACS (BD FACSAria). For routine culture, rat arterial endothelial cells were cultured in M199 with 15% fetal bovine serum (FBS). For routine culture, mouse neonatal cardiac fibroblasts were cultured in DMEM-HG with 10% FBS. During coculture experiments, ECs/FBs were cultured with ESC-CMs in DMEM-LG with 2% FBS. ESC-CMs were cultured 1:1 with ECs or cardiac fibroblasts pre-plated 1 day earlier (Hsieh et al., 2006b).

Exiqon miRNA Microarray

For each array, 1 μg of total RNA was labeled with Hy3 or Hy5 using the miRCURY LNA microRNA Array Labeling Kit (Exiqon). Fluorescently labeled RNA was hybridized to Exiqon miRCURY LNA miRNA arrays (v.11.0) (human, mouse, and rat) (Exiqon) for 16 hr at 56°C using a MAUI DNA microarray hybridization station and SL mixer (BioMicro Systems). Arrays were washed and scanned on an Axon GenePix 4000B scanner (Molecular Devices), and GenePix results (GPR) files containing fluorescence intensities were generated using GenePix Pro (v.6.0) (Molecular Devices) software. GPR files were loaded into GeneSpring (v.11.5) (Agilent Technologies) and normalized using the global Lowess algorithm. Flagged spots were removed from subsequent analysis. These microarray data are deposited at GEO: GSE69927.

Transient Transfection

ESC-CMs at 60%–70% confluence were transfected with pre-miR-125b, pre-miR-199a, pre-miR-221, pre-miR-222 (PM10148, PM10893, PM10337, and PM11376, respectively), or a negative control (scramble; 25 nM) using

Pepmute as a transfection agent. For ErbB4 inhibition, siErbB4-1 and siErbB4-2 (s201303, ss201304; Ambion) were compared to a negative control using the same transfection agent (25 nM).

Cardiac Differentiation and Culture of Human ESCs

Protocols were approved by the Academia Sinica Institutional Review Board. H9 cells were routinely maintained and expanded in feeder-free conditions on Matrigel-coated plates using mouse-embryonic-fibroblast-conditioned medium with 5 ng/ml bFGF. Prior to cardiac differentiation, cells were plated at a density of 150,000 cells/cm^2. To induce cardiac differentiation, media was replaced with RPMI-B27-insulin and 100 ng/ml recombinant human Activin A. After 24 hr, medium was changed to RPMI-B27-insulin with BMP-4 and Wnt agonist CHIR99021. 2 days later, the medium was switched to Wnt antagonist Xav 939 (Yang et al., 2014b). Initial beating was typically observed approximately 10 days post-induction. Only cell preparations containing >80% cardiac troponin T-positive cardiomyocytes were used for further experiments.

Data Analysis

Data are expressed as mean ± SEM. Statistical significance was determined using a two-tailed Student's t test or ANOVA, as appropriate. Differences between groups were considered statistically significant at p values of less than 0.05.

ACCESSION NUMBERS

The accession numbers for the *miRNA* and *ErbB4* siRNA microarray data reported in this paper are GEO: GSE69927 and GEO: GSE69897.

SUPPLEMENTAL INFORMATION

Supplemental Information includes Supplemental Experimental Procedures and four figures and can be found with this article online at http://dx.doi.org/10.1016/j.celrep.2015.08.042.

AUTHOR CONTRIBUTIONS

Conceptualization, D.S.L., J.-H.C., and P.C.H.H.; Methodology, D.S.L., R.-C.S., C.-C.C., C.E.M., and P.C.H.H.; Investigation, D.S.L. and C.H.L.; Writing – Original Draft, D.S.L., D.J.L., and P.C.H.H.; Writing – Review & Editing, D.S.L., D.J.L., L.P., S.C., C.E.M., and P.C.H.H.; Resources, R.C.S., C.-C.C., S.-N.W., and C.E.M.; Supervision, S.-M.H., Y.-T.Y, S.-T.L., P.-M.C., S.C., C.E.M., J.-H.C. and P.C.H.H.; Funding Acquisition, J.H.C. and P.C.H.H.

ACKNOWLEDGMENTS

This work was supported by the National Research Program for Biopharmaceuticals of the Ministry of Science and Technology (MOST; 102-2321-B-001-069, 104-2325-B-001-010, and 102-2314-B-039-032) and the Academia Sinica Translational Medicine Program. The Exiqon miRNA microarray assays were performed by the DNA Microarray Core Laboratory at the Institute of Plant and Microbial Biology, Academia Sinica, Taiwan. The authors thank Mr. James Fugate for providing expert training in human cardiac differentiation methods.

Received: March 1, 2015
Revised: June 22, 2015
Accepted: August 12, 2015
Published: September 10, 2015

REFERENCES

Bersell, K., Arab, S., Haring, B., and Kühn, B. (2009). Neuregulin1/ErbB4 signaling induces cardiomyocyte proliferation and repair of heart injury. Cell *138*, 257–270.

Blum, B., Hrvatin, S.S., Schuetz, C., Bonal, C., Rezania, A., and Melton, D.A. (2012). Functional beta-cell maturation is marked by an increased glucose threshold and by expression of urocortin 3. Nat. Biotechnol. *30*, 261–264.

Brutsaert, D.L. (2003). Cardiac endothelial-myocardial signaling: its role in cardiac growth, contractile performance, and rhythmicity. Physiol. Rev. *83*, 59–115.

Cardinali, B., Castellani, L., Fasanaro, P., Basso, A., Alemà, S., Martelli, F., and Falcone, G. (2009). Microrna-221 and microrna-222 modulate differentiation and maturation of skeletal muscle cells. PLoS ONE *4*, e7607.

Cordes, K.R., and Srivastava, D. (2009). MicroRNA regulation of cardiovascular development. Circ. Res. *104*, 724–732.

Ge, Y., Sun, Y., and Chen, J. (2011). IGF-II is regulated by microRNA-125b in skeletal myogenesis. J. Cell Biol. *192*, 69–81.

Hsieh, P.C.H., Davis, M.E., Lisowski, L.K., and Lee, R.T. (2006a). Endothelial-cardiomyocyte interactions in cardiac development and repair. Annu. Rev. Physiol. *68*, 51–66.

Hsieh, P.C.H., MacGillivray, C., Gannon, J., Cruz, F.U., and Lee, R.T. (2006b). Local controlled intramyocardial delivery of platelet-derived growth factor improves postinfarction ventricular function without pulmonary toxicity. Circulation *114*, 637–644.

Hu, S., Huang, M., Nguyen, P.K., Gong, Y., Li, Z., Jia, F., Lan, F., Liu, J., Nag, D., Robbins, R.C., and Wu, J.C. (2011). Novel microRNA prosurvival cocktail for improving engraftment and function of cardiac progenitor cell transplantation. Circulation *124* (*Suppl 11*), S27–S34.

Katakowski, M., Buller, B., Wang, X., Rogers, T., and Chopp, M. (2010). Functional microRNA is transferred between glioma cells. Cancer Res. *70*, 8259–8263.

Kim, C., Majdi, M., Xia, P., Wei, K.A., Talantova, M., Spiering, S., Nelson, B., Mercola, M., and Chen, H.S. (2010). Non-cardiomyocytes influence the electrophysiological maturation of human embryonic stem cell-derived cardiomyocytes during differentiation. Stem Cells Dev. *19*, 783–795.

Kim, C., Wong, J., Wen, J., Wang, S., Wang, C., Spiering, S., Kan, N.G., Forcales, S., Puri, P.L., Leone, T.C., et al. (2013). Studying arrhythmogenic right ventricular dysplasia with patient-specific iPSCs. Nature *494*, 105–110.

Kuppusamy, K.T., Jones, D.C., Sperber, H., Madan, A., Fischer, K.A., Rodriguez, M.L., Pabon, L., Zhu, W.-Z., Tulloch, N.L., Yang, X., et al. (2015). Let-7 family of microRNA is required for maturation and adult-like metabolism in stem cell-derived cardiomyocytes. Proc. Natl. Acad. Sci. USA *112*, E2785–E2794.

Laflamme, M.A., and Murry, C.E. (2005). Regenerating the heart. Nat. Biotechnol. *23*, 845–856.

Lloyd-Jones, D., Adams, R.J., Brown, T.M., Carnethon, M., Dai, S., De Simone, G., Ferguson, T.B., Ford, E., Furie, K., Gillespie, C., et al.; American Heart Association Statistics Committee and Stroke Statistics Subcommittee (2010). Executive summary: heart disease and stroke statistics–2010 update: a report from the American Heart Association. Circulation *121*, 948–954.

Lompré, A.M., Nadal-Ginard, B., and Mahdavi, V. (1984). Expression of the cardiac ventricular alpha- and beta-myosin heavy chain genes is developmentally and hormonally regulated. J. Biol. Chem. *259*, 6437–6446.

Maroof, A.M., Keros, S., Tyson, J.A., Ying, S.W., Ganat, Y.M., Merkle, F.T., Liu, B., Goulburn, A., Stanley, E.G., Elefanty, A.G., et al. (2013). Directed differentiation and functional maturation of cortical interneurons from human embryonic stem cells. Cell Stem Cell *12*, 559–572.

Miyoshi, N., Ishii, H., Nagano, H., Haraguchi, N., Dewi, D.L., Kano, Y., Nishikawa, S., Tanemura, M., Mimori, K., Tanaka, F., et al. (2011). Reprogramming of mouse and human cells to pluripotency using mature microRNAs. Cell Stem Cell *8*, 633–638.

Navarrete, E.G., Liang, P., Lan, F., Sanchez-Freire, V., Simmons, C., Gong, T., Sharma, A., Burridge, P.W., Patlolla, B., Lee, A.S., et al. (2013). Screening drug-induced arrhythmia [corrected] using human induced pluripotent stem cell-derived cardiomyocytes and low-impedance microelectrode arrays. Circulation *128* (*11 Suppl 1*), S3–S13.

Nunes, S.S., Miklas, J.W., Liu, J., Aschar-Sobbi, R., Xiao, Y., Zhang, B., Jiang, J., Massé, S., Gagliardi, M., Hsieh, A., et al. (2013). Biowire: a platform for maturation of human pluripotent stem cell-derived cardiomyocytes. Nat. Methods *10*, 781–787.

Peters, N.S., Severs, N.J., Rothery, S.M., Lincoln, C., Yacoub, M.H., and Green, C.R. (1994). Spatiotemporal relation between gap junctions and fascia adherens junctions during postnatal development of human ventricular myocardium. Circulation *90*, 713–725.

Small, E.M., Frost, R.J.A., and Olson, E.N. (2010). MicroRNAs add a new dimension to cardiovascular disease. Circulation *121*, 1022–1032.

Takahashi, T., Lord, B., Schulze, P.C., Fryer, R.M., Sarang, S.S., Gullans, S.R., and Lee, R.T. (2003). Ascorbic acid enhances differentiation of embryonic stem cells into cardiac myocytes. Circulation *107*, 1912–1916.

van Rooij, E., Sutherland, L.B., Liu, N., Williams, A.H., McAnally, J., Gerard, R.D., Richardson, J.A., and Olson, E.N. (2006). A signature pattern of stress-responsive microRNAs that can evoke cardiac hypertrophy and heart failure. Proc. Natl. Acad. Sci. USA *103*, 18255–18260.

Wong, S.S.Y., Ritner, C., Ramachandran, S., Aurigui, J., Pitt, C., Chandra, P., Ling, V.B., Yabut, O., and Bernstein, H.S. (2012). miR-125b promotes early germ layer specification through Lin28/let-7d and preferential differentiation of mesoderm in human embryonic stem cells. PLoS ONE *7*, e36121.

Yang, X., Pabon, L., and Murry, C.E. (2014a). Engineering adolescence: maturation of human pluripotent stem cell-derived cardiomyocytes. Circ. Res. *114*, 511–523.

Yang, X., Rodriguez, M., Pabon, L., Fischer, K.A., Reinecke, H., Regnier, M., Sniadecki, N.J., Ruohola-Baker, H., and Murry, C.E. (2014b). Tri-iodo-l-thyronine promotes the maturation of human cardiomyocytes-derived from induced pluripotent stem cells. J. Mol. Cell. Cardiol. *72*, 296–304.

Zhang, Y., Li, S., Yuan, L., Tian, Y., Weidenfeld, J., Yang, J., Liu, F., Chokas, A.L., and Morrisey, E.E. (2010). Foxp1 coordinates cardiomyocyte proliferation through both cell-autonomous and nonautonomous mechanisms. Genes Dev. *24*, 1746–1757.

Zhao, Y.-Y., Feron, O., Dessy, C., Han, X., Marchionni, M.A., and Kelly, R.A. (1999). Neuregulin signaling in the heart. Dynamic targeting of erbB4 to caveolar microdomains in cardiac myocytes. Circ. Res. *84*, 1380–1387.

Ziman, A.P., Gómez-Viquez, N.L., Bloch, R.J., and Lederer, W.J. (2010). Excitation-contraction coupling changes during postnatal cardiac development. J. Mol. Cell. Cardiol. *48*, 379–386.